sciendo

Substitution effect of phenol derivatives on electrochemical oxidation potentials: Correlation of theoretical reaction Gibbs free energies

Andrea Kováčová

Institute of Physical Chemistry and Chemical Physics, Slovak University of Technology in Bratislava, Radlinského 9, SK-812 37 Bratislava, Slovakia
andrea.kovacova@stuba.sk

Abstract: Reaction Gibbs free energies for electron abstraction from phenol and its 74 derivatives were calculated using the composite *ab-initio* approach (G4) in combination with the implicit solvation model. Resulting values were correlated with 38 oxidation potentials obtained from cyclic voltammetry measurements. Substitution effect and the role of substituents in *ortho*-, *meta*-, and *para*-position were also quantified by Hammett constants. The evaluated linear dependences can be used to reliably estimate electrochemical potentials of substituted phenols solvated in water.

Keywords: Reaction Gibbs energies; Gn approach; Thermodynamics; Implicit solvent model

Introduction

Phenol and its derivatives are key moieties in the production of polycarbonates, detergents, herbicides, synthetic drugs, dyes, and antioxidants. Phenolic structural units are also widely distributed in plants and they play important roles in living systems, such as defence mechanisms against viruses, bacteria (Albuquerque et al., 2021) or reactive radicals (Michalík et al., 2019a). Phenolic compounds can also represent hazardous industrial pollutants (Guerra, 2001). On the other hand, chelating ability of polyphenols (Michalík et al., 2021; Šimunková et al., 2022) can potentially be used to eliminate solvated metal ions in wastewater. The main chemical transformation pathway of these molecules is often associated with their oxidation where electron loss can occur electrochemically (Pavitt et al., 2017) or in the presence of reducing metal cations (Ignaczak et al., 1987).

Theoretical calculations using quantum chemical methods play a very important role in this context; although they do not always provide accurate absolute values of quantities, they correctly reproduce experimental trends. Structural or energetic parameters of phenol-based molecules can also be correlated with biological activity (Štellerová et al., 2022). Currently, Density Functional Theory (DFT) calculations are most commonly used due to their lower computational cost. However, chemical accuracy of the results depends on the choice of DFT functional and the basis set. In case of thermochemical data calculations, the Gaussian-n (Gn) method is generally more accurate as it is based on a series of calculations using different methods and basis sets to obtain accurate energetics (Curtiss et al., 2007). In addition, various molecule-specific empirically independent parameters and higher-level correction terms are included to estimate the remaining deficiencies, assuming they are systematic (Curtiss et al., 2007). The use of geometries and zero-point energies from the DFT, application of CCSD(T) energies, inclusion of estimated *ab initio* Hartree-Fock limit energy, and addition of higher level correction parameters in the G4 method contribute to the most significant improvement of the original Gn theory (Curtiss et al., 2007). The combination of the implicit solvent model with G4 or DFT has been successfully used to predict the reaction enthalpies and Gibbs energies of phenol and its analogues (Cagardová et al., 2019; Michalík et al., 2019a; Biela et al., 2023). Interestingly, the use of pure *ab initio* MPn approach can fail in the theoretical prediction of bond dissociation enthalpies (Klein and Lukeš, 2006).

Description of solvent-solute effects can significantly affect the quality of the results obtained. Inclusion of explicit solvent molecules surrounding the molecule under investigation generates numerous geometry structures and consequently leads to rapid increase of computational time. The use of implicit solvent approximation assumes that solvent molecules can be replaced by a homogeneously polarisable and thermally averaged isotropic medium (Mennucci et al., 2002). Many theoretical physicochemical properties calculated for flavonols (Michalík et al., 2019b), phenols (Michalík et al., 2017), alcohols (Michalík and Lukeš, 2016), model amines (Rimarčík et al., 2010), and toluidine isomers (Lukeš and Hartmann, 2021) solvated in different polar solvents are reasonably well estimated using implicit solvent models combined with DFT.

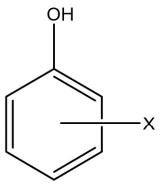

X: H, NMe_2, F, Br, CF_3, NO, COH, Me, Et, OMe, NO_2, Ph, Cl, OH, CN, COMe, COOH, NH_2

a)

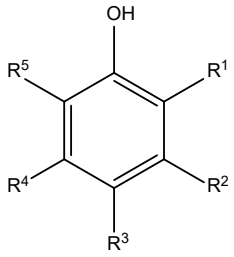

Name	Notation	Name	Notation
2,3-dimethylphenol	23Me	3,4-dimethoxyphenol	34OMe
2,4-dimethylphenol	24Me	3,5-dimethoxyphenol	35OMe
2,5-dimethylphenol	25Me	2,4-dinitrophenol	$24NO_2$
2,6-dimethylphenol	26Me	dopamine	dopamine
3,4-dimethylphenol	34Me	2,4,6-trimethylphenol	246Me
3,5-dimethylphenol	35Me	2,4,6-trichlorophenol	246Cl
2,3-dimethoxyphenol	23OMe	2-methoxy-4-ethylphenol	2OMe-4Et
2,4-dimethoxyphenol	24OMe	2-Hydroxy-4-methoxybenzaldehyde	2OMe-4COH
2,5-dimethoxyphenol	25OMe	2,4-dinitro-2-methylphenol	$2Me\text{-}24NO_2$
2,6-dimethoxyphenol	26OMe	2,6-dinitro-4-methylphenol	$4Me\text{-}26NO_2$

(b)

Fig. 1. Schematic structures and notations of studied molecules (a) mono- (b) polysubstitued.

Satisfactory predictions were also obtained for hydroxyl groups attached to non-aromatic rings (Žemlička et al., 2014) and alkyl chains (Štellerová and Lukeš, 2021).

One-electron oxidation reactions of phenols can affect various types of chemical processes. Therefore, knowledge of electrochemical properties of these compounds is crucial for the identification of these reactions. In this context, experimental study by Pavitt et al. (2017) is interesting, where half-wave oxidation potentials ($E_{1/2}$) were measured and determined electrochemically for a series of 38 phenol derivatives in water and isopropyl alcohol. These electrochemical potentials were correlated with calculated DFT potentials; solvent effects were included using the COSMO and SMD models. Although a relatively large number of substances have been studied experimentally, the role of substitution has not been sufficiently discussed. In particular, the electron-donating or electron-withdrawing effect of the substituent as well as the role of the substituent position have not been sufficiently addressed. Therefore, partial aims of this study include: (1) calculation of G4 reaction Gibbs free energies of the reaction between radical cations and neutral molecules; (2) analysis of the substituent effect using Hammett constants; (3) correlation of obtained data with available experimental $E_{1/2}$ values. In this study, 74 derivatives have been investigated (Fig. 1).

Computational Details

Quantum chemical calculations in water were performed at Gaussian-4 level (G4) of theory (Curtiss et al., 2007), which selects a suitable basis set, e.g. in this work, the GTBas3 basis set, i.e. 6-31G(2df,p) for molecules containing H, C, N, F, Cl, and 6-31G(2fg) for molecules possessing Br atom. Contributions of the solvent effect were approximated by the SMD model (Solvation Model based on the quantum mechanical charge Density of a solute molecule interacting with a continuum) (Marenich et al., 2009), which is based on generalised Born equation represented by an approximation of the Poisson equation suitable for arbitrary cavity shapes. Gibbs free energies were evaluated for the temperature of 298.15 K and the pressure of 101.325 kPa. Calculations were performed using the Gaussian 09 software (Frisch et al., 2009). Vibrational analysis included in the G4 calculation process showed no imaginary frequencies, confirming the geometry corresponding to the lowest energy minimum. From the optimal geometries obtained for all studied molecules, optimal geometries of the *ortho*- and polysubstituted phenol derivatives were visualised using the Jmol viewer (Fig. 2) (Jmol development team, 2016). In this work, the type of reaction studied is presented in Eq. (1)

$$X—Ar—OH \rightarrow (X—Ar—OH)^{\bullet+} + e^- \qquad (1)$$

where X represents the substituents used. Spin state of neutral compounds is a singlet and corresponding cation radicals consist of one unpaired electron, i.e., their spin state is doublet.

Reaction Gibbs free energies expressing electron abstraction ($\Delta_r G^e$) are

$$\Delta_r G^e = G((X—Ar—OH)^{\bullet+}) - G(X—Ar—OH) + G(e^-) = \\ = \Delta G + G(e^-) \qquad (2)$$

where $G((X—Ar—OH)^{\bullet+})$ and $G(X—Ar—OH)$ denote the Gibbs free energies of the cation radical and neutral compound, respectively, and $G(e^-)$ is the Gibbs free energy of the solvated electron. The value of $G(e^-)$ is constant for all reactions and it is deduced from linear dependences (see the intercept of Eq. 6). For this reason, all energy values in this manuscript are given without the value of $G(e^-)$. According to the thermodynamic theory (Atkins and Paula, 2006), the absolute electrochemical potential can be calculated from the reaction Gibbs energies using the equation

$$E = -\Delta_r G^e / nF \quad (3)$$

where E denotes the electrochemical potential, $\Delta_r G^e$ is the reaction Gibbs free energy, n represents the number of exchange electrons in the reaction, and F is the Faraday constant (96 485 $C \cdot mol^{-1}$). Assuming that the absolute electrochemical potential of the Standard Hydrogen Electrode (SHE) is 4.28 V (E^{SHE}), according to (Ho et al., 2016), the value of the electrochemical potential is calculated as follows

$$E^{cal} = E - E^{SHE} \quad (4)$$

In our study, the dependence between the available Hammett constants (Tab. 1) and the experimental values of the electrochemical potentials for *ortho*, *meta* and *para* derivatives has been examined (Fig. 3).

Tab. 1. Takahata-Chong Hammett type constants for *ortho* isomers (σ_o) (Takahata and Chong, 2005) and Hammett constants for *meta* (σ_m) and *para* (σ_{p^+}) isomers (Hansch et al., 1991).

Substituent	σ_o	σ_m	σ_{p^+}
H	0.00	0.00	0.00
Me	–0.17	–0.07	–0.31
Et	–0.31	–0.07	–0.30
OMe	–0.39	0.12	–0.78
NO_2	0.80	0.71	0.79
Ph		0.06	–0.18
Cl	0.20	0.37	0.11
OH	–0.05	0.12	–0.92
CN	0.71	0.56	0.66
COMe		0.38	
COOH		0.37	0.42
NH_2	–0.41	–0.16	–1.30
COH		0.35	0.73
F	0.24	0.34	–0.07
Br		0.39	0.15
CF_3		0.43	0.61
NO		0.62	
NMe_2	–0.73	–0.16	–1.70

Results and discussion

Optimised geometries of selected species from the studied molecules are shown in Fig. 2. The phenolic group and the substituents are in one plane with the benzene ring. Exceptions are sterically bulky substituents such as **Ph, bisphenol A** and **NMe_2**. In case of *ortho*-substituents containing oxygen or halogen atoms, an intramolecular hydrogen bond is formed with the **OH** group.

Calculated ΔG values for aqueous environment are listed in Tab. 3 and Tab. 4. The reaction Gibbs free energies range from 473 $kJ \cdot mol^{-1}$ for **$4NMe_2$** to 672 $kJ \cdot mol^{-1}$ for **$24NO_2$** and their values indicate that the reactions are exothermic in the reduction direction.

Results obtained from the theoretical G4 reaction Gibbs energies are summarised in Tab. 3 and Tab. 4; a comparison of the theoretical values with the available experimental values indicates large deviations. The values range from 0.33 for **3Cl** to 1.19 for **$4NH_2$**. For example, for **$4NH_2$**, the experimental value is 0.425 V vs. SHE and the theoretical value is –0.77 V. A possible explanation is related to the limitations of both the implicit model and the DFT approach.

In physical organic chemistry, Hammett constants are used to estimate the substitution effect of aromatic molecules. This approach provides a simple way of determining the electron-donating (negative values) and electron-withdrawing (positive values) groups, respectively. They are different for *meta* (σ_m) and *para* (σ_p) substituents, i.e., a substituent can be electron-withdrawing in the *meta* position and electron-donating in the *para* position, e.g., **Ph**, **F**, **OCH_3**. For *ortho* substituents, there are several *Hammett-type substituent constants* (σ_o), e.g., the **Takahata constants** (Takahata & Chong, 2005). For *para* substituents, in addition to σ_p, there are also the Brown-Okamoto constants (σ_{p^+} and σ_{p^-}) (Brown and Okamoto, 1957), the use of which depends on the reaction centre of the molecule. Therefore, Hammett constants have long been used for different types of dependences where it is necessary to find a relationship between different types of substituents and a given quantity (e.g., BDE, ionisation potentials, pK_a) (Bordwell et al., 1994; Klein et al., 2009; Lukeš et al., 2017). The *ortho* Hammett constants proposed by Takahata are not available for all substituents (Takahata and Chong, 2005).

The dependence of Hammett constants (σ) on the experimental electrochemical potentials (E) is linear

$$E/V = 0.377 \times \sigma_{o,m,p^+} - 1.016 \quad (5)$$

with the coefficient of determination (R^2) of 0.918 (Fig. 3). Errors of the regression parameters

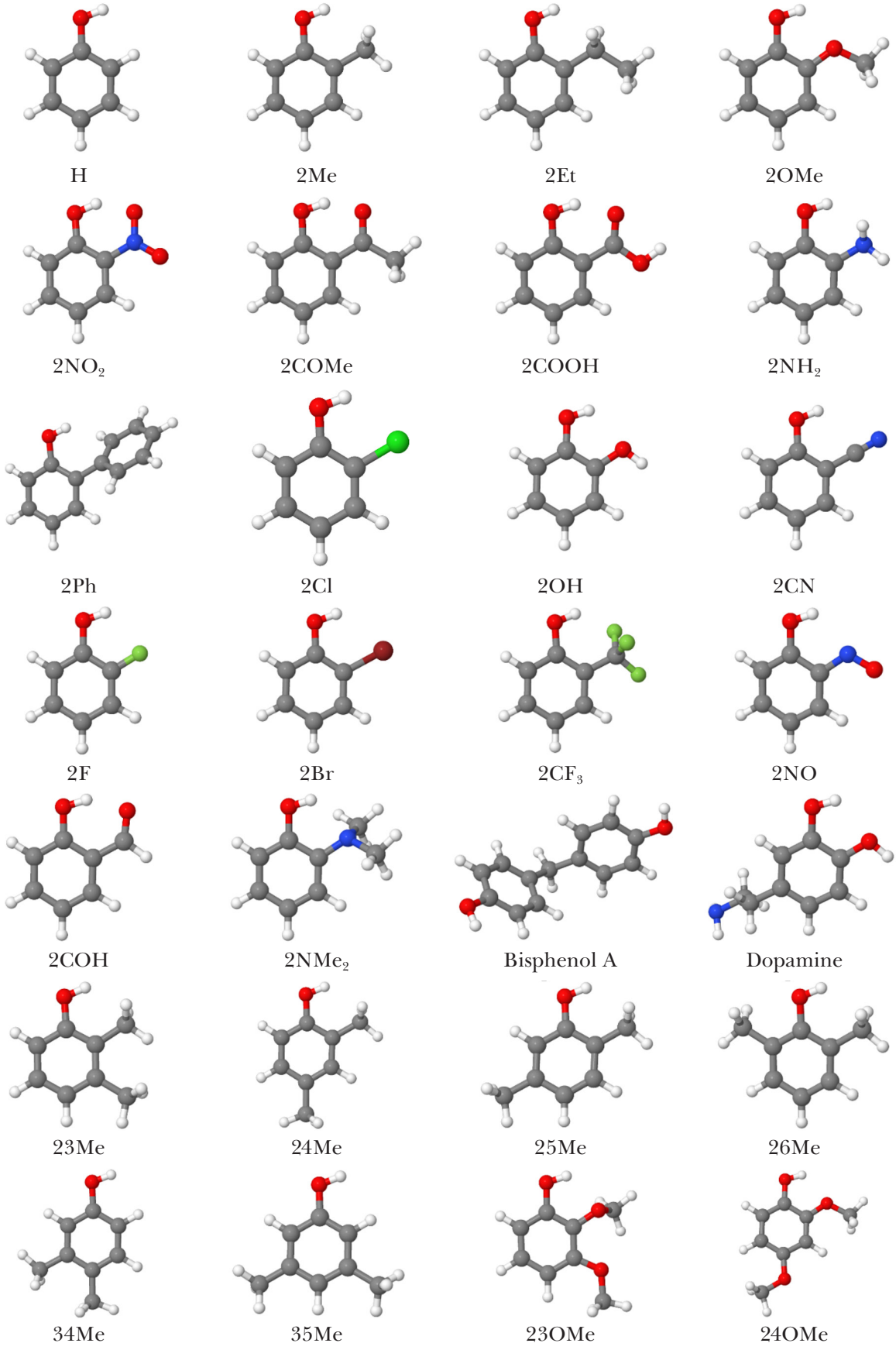

Fig. 2a. Optimal geometries of neutral forms of studied *ortho*- and poly-substituted species in aqueous solution.

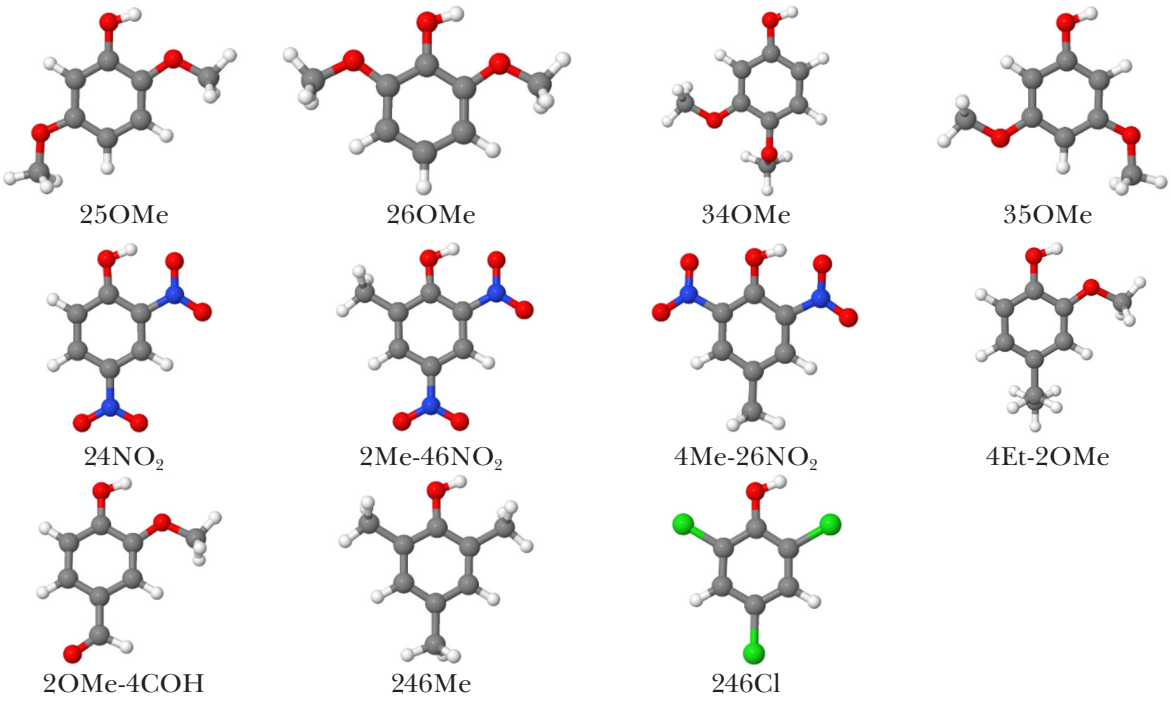

Fig. 2b. Optimal geometries of neutral forms of studied *ortho*- and poly-substituted species in aqueous solution.

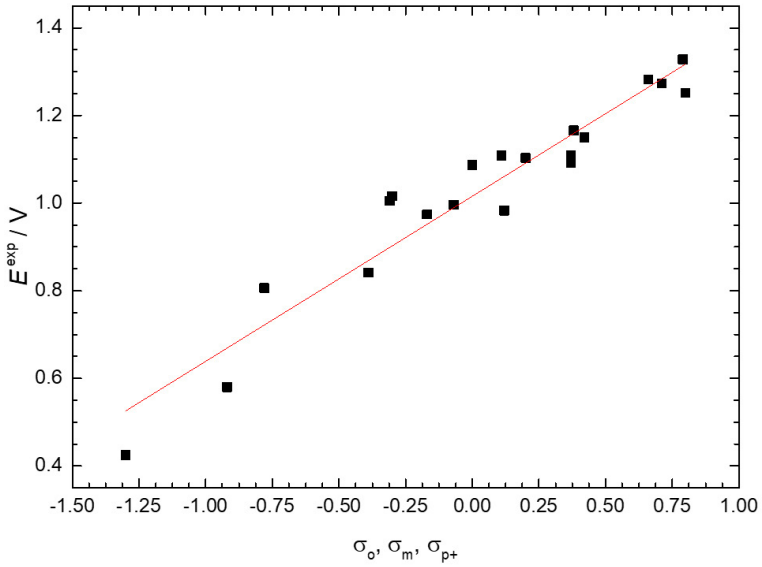

Fig. 3. Correlation between Hammett (Hansch et al., 1991; Takahata and Chong, 2005) and available experimental electrochemical potential values (Pavitt et al., 2017) for studied species in water.

are 0.015 V for intercept and 0.026 V for slope, respectively. In case of *para* substituents, σ_{p+} constants were used in the linear dependence since the dependence employing σ_p and σ_{p-} constants, respectively, showed worse correlation. For compounds with more substituents or where Hammett constants are not available, the correlation between Hammett constants and experimental electrochemical potential cannot be reliably evaluated.

Shortcomings of the theoretical model used can be overcome by direct correlation of the available electrochemical oxidation potentials $E_{1/2}$ with the calculated ΔG. As it is shown in Fig. 4, this correlation is linear and can be described by the following equation

$$E/\mathrm{V} = 0.005 \times \Delta G/\mathrm{kJ \cdot mol^{-1}} - 2.174 \qquad (6)$$

with a satisfactory value of coefficient of determi-

Tab. 2. Parameters a, b with errors and coefficient of determination (R^2) for linear correlations described by the equation $E/V = a \times \Delta G/kJ \cdot mol^{-1} - b$ for *ortho-* with polysubstitueted phenols (E_o), *meta-* (E_m) and *para-* (E_p) substituted phenols.

	$a\ 10^{-3}/mol \cdot V \cdot kJ^{-1}$	b/V	$\sigma_a\ 10^{-4}/mol \cdot V \cdot kJ^{-1}$	σ_b/V	R^2
E_o	5.5	–2.18	2.4	0.15	0.977
E_m	4.2	–1.41	9.1	0.54	0.773
E_p	5.8	–2.36	3.9	0.23	0.958

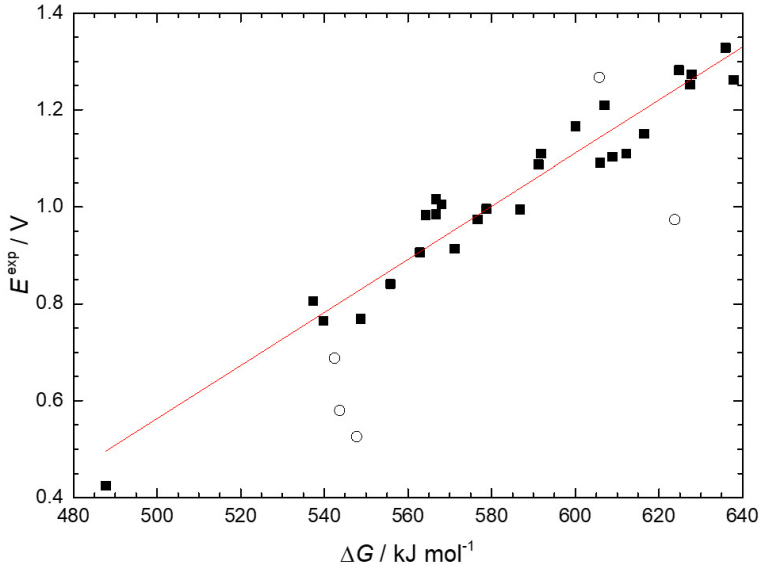

Fig. 4. Correlation between the difference in Gibbs energies of the cation radical forms and neutral molecules and the available experimental electrochemical potential values (Pavitt et al., 2017) for studied species in water. Open circles represent groups excluded from the linear regression.

nation, $R^2 = 0.953$, for studied derivatives. Errors of the regression parameters are 0.14 V for intercept and 2.3 10^{-4} $mol \cdot V \cdot kJ^{-1}$ for slope, respectively. In addition to this correlation, correlations were also performed separately for *ortho-* with polysubstituted phenols (E_o), *meta-* (E_m) and *para-* (E_p) substituted phenols separately. Regression parameters *a*, *b* with the regression errors and the coefficient of determination (R^2) obtained from these linear correlations are summarised in Tab. 2. In these regressions, the same points were excluded from the joint correlation. As the regressions contain different numbers of points, our calculations are based on Eq. 6.

The intercept includes $G(e^-)$, which has a value of $-149\ kJ \cdot mol^{-1}$ (Zhan and Dixon, 2003; Fifen, 2013), while the slope covers the imperfections of the implicit model for the specified type of substituted molecules. Based on the correlation coefficient, experimental values of electrochemical potentials are in good agreement with our calculated Gibbs energies. All 36 experimental values of the electrochemical potential were available for the studied compounds (6 for *ortho-* and *meta-*substituted, 11 for *para-*substituted, and 9 for polysubstituted derivatives). Some substituents had to be excluded from the correlation (Fig. 4) because they did not follow the general trend and were significantly scattered from the regression line. **2COOH** shows a slight deviation from the linear dependence due to steric effects occurring in phenolic derivatives with substituents in the *ortho* position between the substituent and the OH group, but also due to expected dissociation of the **COOH** group. Thus, it is possible that the available experimental value of the electrochemical potential for compounds containing the **COOH** group belongs to its carboxylate anion. Deviations from the linear dependence were also observed for **4OH**, **26OMe**, **246Cl,** and **dopamine** (Fig. 4).

Estimated electrochemical potentials (E) corresponding to the oxidation of all phenolic derivatives studied based on these equations are summarised in Tab. 3 and Tab. 4. The Gibbs energies and associated electrochemical potentials range from 509 $kJ \cdot mol^{-1}$ (0.61 V) for **2NMe$_2$** to 627 $kJ \cdot mol^{-1}$ (1.26 V) for **2NO$_2$**, from 496 $kJ \cdot mol^{-1}$ (0.54 V) for **3NMe$_2$** to 628 $kJ \cdot mol^{-1}$ (1.26 V) for **3NO$_2$**, from 473 $kJ \cdot mol^{-1}$ (0.41 V) for **4NMe$_2$** to 636 $kJ \cdot mol^{-1}$

Tab. 3. Calculated G4(SMD=water) Gibbs free energies (ΔG) in kJ · mol^{-1} for electron abstraction, electrochemical potential values calculated from Eq. 4 vs. SHE, scaled electrochemical potential values obtained from Eqs. 5—6 in V, and experimental electrochemical potential E vs. SHE (Pavitt et al., 2017). Values in parentheses stand for the Gibbs reaction energies for electron abstraction evaluated from electrochemical potentials (Eq. 3).

Substituent	*ortho*					*meta*					*para*				
	ΔG	E^{cal}	$E^{\Delta G}$	E^{σ}	E^{exp}	ΔG	E^{cal}	$E^{\Delta G}$	E^{σ}	E^{exp}	ΔG	E^{cal}	$E^{\Delta G}$	E^{σ}	E^{exp}
H	591	0.30	1.06 (102)	1.02	1.09	591	0.30	1.06 (102)	1.02	1.09	591	0.30	1.06 (102)	1.02	1.09
Me	577	0.15	0.98 (95)	0.95	0.97	579	0.17	0.99 (96)	0.99	1.00	568	0.06	0.93 (90)	0.90	1.01
Et	580	0.19	1.00 (97)	0.90		576	0.15	0.98 (94)	0.99		567	0.05	0.93 (89)	0.90	1.02
OMe	556	–0.06	0.87 (84)	0.87	0.84	564	0.02	0.91 (88)	1.06	0.98	537	–0.25	0.77 (74)	0.72	0.81
NO_2	627	0.68	1.26 (121)	1.32	1.25	628	0.68	1.26 (122)	1.28	1.27	636	0.77	1.30 (126)	1.31	1.33
Ph	587	0.26	1.04 (100)	1.02	1.00	583	0.22	1.02 (98)	1.04		562	0.00	0.90 (87)	0.95	
Cl	609	0.49	1.16 (112)	1.09	1.10	606	0.46	1.14 (110)	1.16	1.09	592	0.31	1.06 (103)	1.06	1.11
OH	563	0.01	0.91 (87)	1.00		574	0.12	0.96 (93)	1.06		544	–0.19	0.80 (77)	0.67	0.58
CN	626	0.67	1.25 (121)	1.28		622	0.62	1.23 (119)	1.23		625	0.65	1.24 (120)	1.26	1.28
COMe	598	0.38	1.10 (106)	1.02		600	0.39	1.11 (107)	1.16	1.17	607	0.47	1.15 (111)	1.02	1.21
COOH	606	0.45	1.14 (110)	1.02	1.27	612	0.52	1.17 (113)	1.16	1.11	616	0.56	1.20 (116)	1.17	1.15
Bisphenol A											571	0.10	0.95 (92)	1.02	0.91
NH_2	515	–0.49	0.64 (62)	0.86		517	–0.46	0.65 (63)	0.96		488	–0.77	0.49 (48)	0.53	0.43
Br	616	0.56	1.20 (115)	1.02		610	0.50	1.17 (112)	1.16		597	0.37	1.09 (106)	1.07	
CF_3	620	0.60	1.22 (118)	1.02		610	0.49	1.16 (112)	1.18		626	0.66	1.25 (121)	1.25	
F	602	0.42	1.12 (108)	1.11		604	0.44	1.13 (109)	1.14		587	0.26	1.04 (100)	0.99	
NMe_2	509	–0.55	0.61 (59)	1.02		496	–0.68	0.54 (52)	0.96		473	–0.92	0.41 (40)	0.37	
NO	592	0.31	1.07 (103)	1.02		590	0.29	1.05 (102)	1.25		576	0.14	0.98 (94)	1.02	
CHO	607	0.46	1.14 (110)	1.02		610	0.50	1.16 (112)	1.15		614	0.54	1.18 (114)	1.29	

(1.30 V) for **4NO$_2$**, and from 521 kJ · mol^{-1} (0.68 V) for **24OMe** to 672 kJ · mol^{-1} (1.14 V) for **24NO$_2$**. The above-mentioned values show that the **NMe$_2$** group has the lowest and **NO$_2$** the highest electrochemical potential for each position in agreement with the corresponding Hammett constants.

As it can be seen from the comparison of the reaction Gibbs energies for cation formation in aqueous

Tab. 4. Calculated G4(SMD=water) Gibbs free energies (ΔG) in kJ · mol^{-1} for electron abstraction, electrochemical potential values calculated from Eq. 4 vs. SHE, scaled electrochemical potential values obtained from Eqs. 5—6 in V, and experimental electrochemical potential E vs. SHE (Pavitt et al., 2017). Values in parentheses stand for the Gibbs reaction energies for electron abstraction evaluated from electrochemical potentials (Eq. 3).

Substituent	ΔG	E^{cal}	$E^{\Delta G}$	E^{exp}	Substituent	ΔG	E^{cal}	$E^{\Delta G}$	E^{exp}
24NO$_2$	672	1.14	1.50 (145)	1.50	**23OMe**	557	–0.05	0.87 (84)	
2Me-46NO$_2$	652	0.93	1.39 (134)	1.40	**24OMe**	521	–0.43	0.68 (65)	
4Me-26NO$_2$	638	0.79	1.32 (127)	1.26	**25OMe**	523	–0.40	0.69 (66)	
Dopamine	548	–0.15	0.82 (79)	0.53	**26OMe**	542	–0.20	0.79 (77)	0.69
23Me	573	0.11	0.96 (93)		**34OMe**	528	–0.35	0.71 (69)	
24Me	556	–0.07	0.86 (83)		**35OMe**	568	0.06	0.93 (90)	
25Me	563	–0.01	0.90 (87)	0.91	**2OMe-4Et**	540	–0.23	0.78 (75)	0.77
26Me	567	0.06	0.93 (90)		**2OMe-4CHO**	567	0.05	0.93 (89)	0.99
34Me	551	–0.12	0.84 (81)		**246Me**	549	–0.14	0.83 (80)	0.77
35Me	568	0.07	0.93 (90)		**246Cl**	624	0.64	1.24 (119)	0.97

Tab. 5. Calculated G4(SMD=water) deprotonation Gibbs free energies ($\Delta_r G$) in kJ · mol^{-1} of proton abstraction for selected molecules calculated according to $\Delta_r G = G$ (deprotonated) — G (protonated) + + G (H^+). Asterisk symbol denotes the molecule with intramolecular hydrogen bond.

Substituent	*ortho*		*meta*		*para*		*poly*	
	$\Delta_r G_1$	$\Delta_r G_2$	$\Delta_r G_1$	$\Delta_r G_1$	$\Delta_r G_1$	$\Delta_r G_2$	$\Delta_r G_1$	$\Delta_r G_2$
OH	87*	102	98	98	106	106		
COOH	34*	99	47	94	51	82		
Bisphenol A					99	99		
Dopamine							90*	102

Tab. 6. Calculated G4(SMD=water) Gibbs free energies (ΔG) in kJ · mol^{-1} for electron abstraction from deprotonated species and scaled electrochemical potential ($E^{\Delta G}$) values obtained from Eq. 6 in V.

Substituent	*ortho*				*meta*				*para*				*poly*			
	ΔG_1	$E^{\Delta G}$	ΔG_2	$E^{\Delta G}$	ΔG_1	$E^{\Delta G}$	ΔG_2	$E^{\Delta G}$	ΔG_1	$E^{\Delta G}$	ΔG_2	$E^{\Delta G}$	ΔG_1	$E^{\Delta G}$	ΔG_2	$E^{\Delta G}$
OH	444	0.25	438	0.22	454	0.31	453	0.30	424	0.14	424	0.14				
COOH	632	1.28			584	1.02			579	0.99						
Bisphenol A									434	0.20	434	0.20				
Dopamine													426	0.16	429	0.17

media, the values range from 40 kJ · mol^{-1} (**4NMe$_2$**) to 145 kJ · mol^{-1} (**24NO$_2$**). In case of molecules with a carboxyl group or an additional hydroxyl group, the hypothetical deprotonated form may also undergo ionisation in aqueous media. This may affect the measurement of the electrochemical potential under investigation. Considering the experimental Gibbs free energy for the proton (–1121 kJ · mol^{-1}) (Tawa et al. 1998; Ishikawa and Nakai 2016), the corresponding reaction Gibbs energies of deprotonation of carboxyl groups are 34 kJ · mol^{-1} (**2COOH**), 47 kJ · mol^{-1} (**3COOH**), and 51 kJ · mol^{-1} (**4COOH**). These values are lower than those of the OH group deprotonation, i.e., 99 kJ · mol^{-1} (**2COOH**), 94 kJ · mol^{-1} (**3COOH**), and 82 kJ · mol^{-1} (**4COOH**). Energetics are influenced by intramolecular hydrogen bonding for the *ortho* position.

In case of molecules containing more than one OH group, the intramolecular hydrogen bonding also affects the reaction energies. Calculated Gibbs deprotonation energies (see Tab. 5) indicate that the energy interval overlaps with the energy interval for the heterolytic cleavage of the O—H bond in hydroxybenzoic acid.

Deprotonation from the hydroxyl group of the **2OH** molecule is energetically more favourable due to stabilisation by an intramolecular hydrogen bond. By abstracting an electron from the anion of the corresponding hydroxybenzoic acid, the ΔG_1 values

change to 632 kJ·mol^{-1} (**2COOH**), 584 kJ·mol^{-1} (**3COOH**), and 579 kJ·mol^{-1} (**4COOH**). Compared to the formation of a cation radical from a neutral molecule, these values are higher for **2COOH** and lower for **3COOH** and **4COOH**. Due to the higher deprotonation energy of the OH group of hydroxybenzoic acid, in comparison with the COOH group, the corresponding electrochemical potentials of the anionic form were not calculated (see Tab. 6).

The corresponding scaled electrochemical potentials for electron abstraction from selected deprotonated species obtained from Eq. 6 are 1.28 V (**2COOH**), 1.02 V (**3COOH**), 0.99 V (**4COOH**) (see Tab. 6). This supports the hypothesis that the experimental potential for **2COOH** can be combined from the values of the two deprotonation processes from the COOH and the OH group. **4OH** and **dopamine** show a lower value of the scaled electrochemical potential when the presence of an anion is assumed. The scaled electrochemical potentials obtained from the deprotonated form in case of **2COOH**, **4OH**, and **dopamine** follow a linear trend compared to the electrochemical potentials obtained from the neutral forms.

Conclusion

In this study, thermodynamics of electron abstraction of phenol and its derivatives has been theoretically investigated. Linear correlation between Hammett constants and calculated Gibbs free energies of the reaction with published experimental electrochemical potentials are presented. Obtained values of electrochemical potentials have an increasing character from electron-donating substituents to electron-accepting substituents, which is in agreement with the corresponding Hammett constants. As the Hammett constants for *ortho* substituents are not available in literature, this approach is only suitable for mono *meta* and *para* substituted derivatives. On the other hand, the correlation between calculated ΔG and experimental E is also possible for *ortho* derivatives. Furthermore, these correlations provided better coefficients of determination than the linear correlations based on the Hammett constants. It can be concluded that the knowledge of calculated ΔG value for polysubstituted phenol in combination with the linear Eq. 6 allows a reliable determination of the scaled electrochemical potential.

Acknowledgement

The work has been supported by the Ministry of Education, Science, Research and Sport of the Slovak Republic, project VEGA 1/0461/21.

References

Albuquerque BR, Heleno SA, Oliveira B, Barros L, Ferreira ICFR (2021) Food Funct. 12: 14–29.

Atkins PW, De Paula J (2006) Atkins' Physical Chemistry. 8th Edition, Oxford University Press, Oxford, New York.

Biela M, Kleinová A, Uhliar M, Klein E (2023) J. Mol. Graph. Model. 122: 1–6.

Bordwell FG, Zhang XM, Satish AV, Cheng JP (1994) J. Am. Chem. Soc. 116: 6605–6610.

Brown HC, Okamoto Y (1957) J. Am. Chem. Soc. 79: 1913–1917.

Cagardová D, Michalík M, Klein E, Lukeš V, Marković Z (2019) Acta Chim. Slovaca 12: 225–240.

Curtiss LA, Redfern PC, Raghavachari K (2007) J. Chem. Phys. 126: 084108.

Fifen JJ (2013) J. Chem. Theory Comput. 9: 3165–3169.

Frisch MJ, Trucks GW, Schlegel HB, GE Scuseria GE, Robb MA, Cheeseman JR, Scalmani G, Barone V, Mennucci B, Petersson GA, Nakatsuji H, Caricato M, Li X, Hratchian HP, Izmaylov AF, Bloino J, Zheng G, Sonnenberg JL, Hada M, Ehara M, Toyota K, Fukuda R, Hasegawa J, Ishida M, Nakajima T, Honda Y, Kitao O, Nakai H, Vreven T, Montgomery JA Jr., Peralta JE, Ogliaro F, Bearpark M, Heyd JJ, Brothers E, Kudin KN, Staroverov VN, Keith T, Kobayashi R, Normand J, Raghavachari K, Rendell A, Burant JC, Iyengar SS,Tomasi J, Cossi M, Rega N, Millam JM, Klene M, Knox JE, Cross JB, Bakken V, Adamo C, Jaramillo J, Gomperts R, Stratmann RE, Yazyev O, Austin AJ, Cammi R, Pomelli C, Ochterski JW, Martin RL, Morokuma K, Zakrzewski VG, Voth GA, Salvador P, Dannenberg JJ, Dapprich S, Daniels AD, Farkas O, Foresman JB, Ortiz JV, Cioslowski J and Fox DJ (2009) Gaussian 09, Revision D.01, Gaussian, Inc. Wallingford CT.

Guerra R (2001) Chemosphere 44: 1737–1747.

Hansch C, Leo A, Taft R (1991) Chem. Rev. 91: 165–195.

Ho J, Coote LM, Cramer CJ, Truhlar DG (2016) Theoretical Calculation of Reduction Potentials. In: Organic Electrochemistry, 5th edn. CRC Press, pp 229–259.

Ignaczak M, Dziegiec' J, Prawicki K (1987) Kinet. Catal. (Engl Transl); (United States) 27(6): 1305–1309.

Ishikawa A, Nakai H (2016) Chem. Phys. Lett. 650: 159–164.

Jmol development team (2016) Jmol: an open-source Java viewer for chemical structures in 3D (14.6). http://jmol.sourceforge.net/.

Klein E, Lukeš V (2006) J. Phys. Chem. A 110: 12312–12320.

Klein E, Rimarčík J, Lukeš V (2009) Acta Chim. Slovaca 2: 37–51.

Lukeš V, Hartmann H (2021) Color. Technol. 137: 389–398.

Lukeš V, Škorňa P, Michalík M, Klein E (2017) Chem. Phys. Lett. 687: 66–72.

Marenich AV, Cramer CJ, Truhlar DG (2009) J. Phys. Chem. B 113: 6378–6396.

Mennucci B, Tomasi J, Cammi R, Cheeseman JR, Frisch MJ, Devlin FJ, Gabriel S, Stephens PJ (2002) J. Phys. Chem. A 106: 6102–6113.

Michalík M, Biela M, Cagardová D, Lukeš V (2021) Chem. Phys. Lett. 762: 138142.

Michalík M, Lukeš V (2016) Acta Chim. Slovaca 9: 89–94.

Michalík M, Poliak P, Lukeš V, Klein E (2019a) Phytochemistry 166: 112077.
Michalík M, Rimarčík J, Lukeš V, Klein E (2019b) Acta Chim. Slovaca 12: 108—118.
Michalík M, Sádecká L, Lukeš V (2017) Acta Chim. Slovaca 10: 91—95.
Pavitt AS, Bylaska EJ, Tratnyek PG (2017) Environ. Sci.: Process Impacts 19: 339—349.
Rimarčík J, Lukeš V, Klein E, Ilčin M (2010) J. Mol. Struct. theochem. 952: 25—30.
Šimunková M, Biela M, Štekláč M, Hlinčík A, Klein E, Malček M (2022) J. Mol. Liq. 359: 119230
Štellerová D, Lukeš V (2021) Acta Chim. Slovaca 14: 32—37.
Štellerová D, Michalík M, Lukeš V (2022) Phytochemistry 203: 113387.
Takahata Y, Chong DP (2005) Int. J. Quantum Chem. 103: 509—515.
Tawa GJ, Topol IA, Burt SK, Caldwell RA, Rashin AA (1998) J. Chem. Phys. 109: 4852—4863.
Žemlička L, Fodran P, Lukeš V, Vagánek A, Slováková M, Staško A, Dubaj T, Liptaj T, Karabín M, Birošová L, Rapta P (2014) Monatsh. Chem. 145: 1307—1318.
Zhan CG, Dixon DA (2003) J. Phys. Chem. B 107: 4403—4417.